

## Chaotic End-State Oscillation of 4H/TSC and WS Fusion

Akito Takahashi

Technova Inc. and Osaka University, Japan

akito@sutv.zaq.ne.jp

**Abstract:** As a model mechanism to explain anomalous excess heat results observed by nano-Ni-H systems, the weak-strong (WS) fusion rate estimation during the unresolved effective life time of end state for the 4H/TSC condensation/collapse motion is of key issue. The effective life of collapsed end state on the order of 1 fs is expected. Computer simulation study was done in this work using the HME-Langevin program, using several key conditions as time-dependent TSC trapping potential, fix-up at 2.4 fm p-p distance of proton hard core collision, and the DDL (deep Dirac level) component effect by relativistic motion of electrons. Computer simulation generated chaotic oscillation of p-p distance of 4H/TSC in the range of 3-100 fm, behaving as near stable (strange attractor) lasting for rather long time ( a few fs or more may be expected).

**Keywords:** 4H/TSC, WS fusion, end state chaotic oscillation, computer simulation, 1 fs life

### 1. Introduction

What is nuclear mechanism of AHE (anomalous heat effect, e.g. 1.5 GJ/mol-H or 15 keV/H) by Ni-H systems [1-3]? The observed AHE data are certainly a circumstantial evidence of non-chemical reaction heat being generated in the interaction of nano-composite metals with hydrogen gas at some elevated temperatures as 200-300 deg C, but it is not yet a direct evidence of identified nuclear reactions. Do we have any rationally proposed theories for possible reaction rate estimation to explain the observed heat level?

The WS (weak-strong) fusion of 4H/TSC<sub>condensation/collapse</sub> is a candidate model [4-6]. To enhance WS fusion rate, life time of collapsed state is of key factor: more than  $1.0E-15$  s (1 fs) is expected. The illustration of [Fig.1](#) is for showing the brief reaction processes. If effective life time of the end state of collapsed 4H/TSC (minimum TSC in [Fig.1-2](#)) will exceed 1 fs, more than 3% of the end state 4H/TSC will make WS fusion via electron capture-to-one-proton, namely neutron generation which makes instantly n-p-p-p 4-body strong interaction. More than 200 W/Mol-H heat power level will be generated by the break-up products ( $^3\text{He}$ , d and p) of  $^4\text{Li}^*$  of intermediate compound

nucleus [4-6].

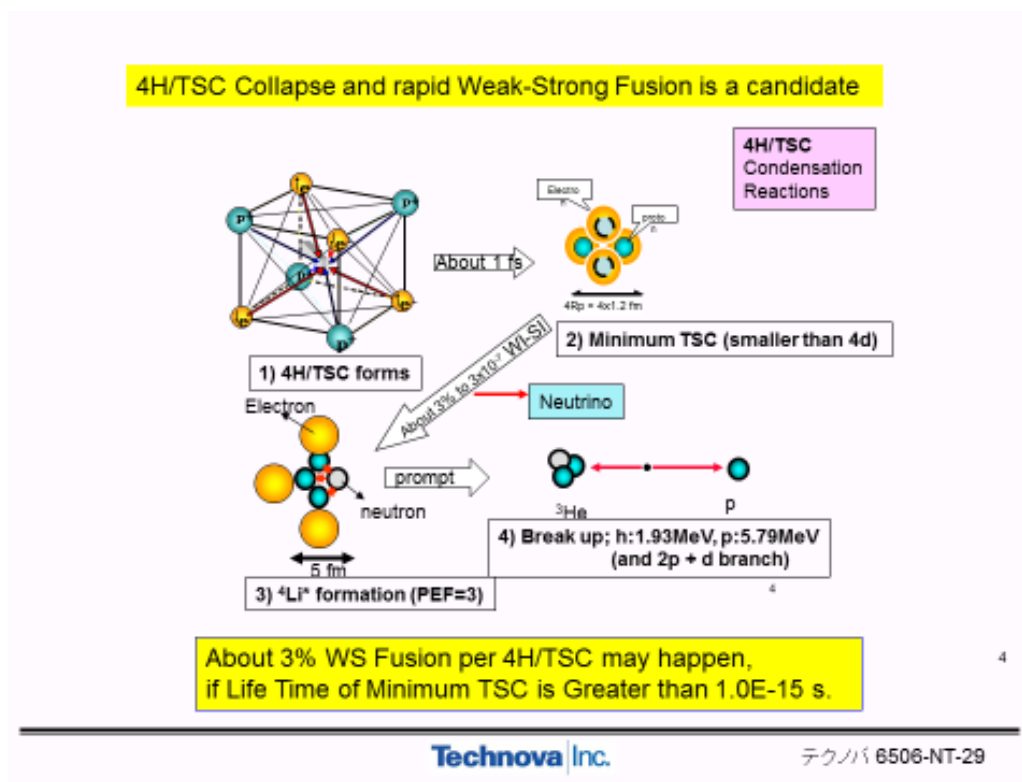


Fig.1: Brief illustration of WS fusion process by 4H/TSC condensation/collapse [4-6]

The 4H/TSC collapse should stop and bounce at  $R_{pp} = 2.4$  fm due to hard core of proton for repulsive strong interaction. What happens after that? Oscillation might be induced? Effective life time of the oscillation end state may be estimated?

In this work, simulation study has been done by modifying the D(H)-Cluster Langevin code [7]. Various conditions were tried for the end-stage of collapse motion:

- 1) Adoption of time dependent pseudo-potentials for TSC trapping
- 2) Fix-up of repulsive p-p state at the collapse end state:  $R_{pp} \geq 2.4$  fm
- 3) Taking relativistic effect for electron state (imitating so called DDL component [8])

Near stable oscillations (may last  $> 1$ fs) were found for 4H/TSC with  $V_{s1}(m, 1.41)$  potentials for a wide band of parameters. However, chaotic behaviors of generating oscillatory motion after the “first” collapse point have been observed in numerical results of simulation, depending on adopted combination of input parameters for the above three conditions. Some detail description is given in the following sections.

## 2. Brief Review of QM-Langevin Treatment

The basic theory is described in references [9, 10, 11, 12]. For reminding very briefly the basic idea and QM (quantum mechanical) physics-mathematical treatment, simplified explanation is given in this section by using some copy of slides at the JCF-16 meeting.

Cold fusion as condensed matter nuclear reaction can take place of observable reaction rate effect in a very microscopic multi-body H(D) trapping potential, for effectively much longer life time of condensation/trapped state [4-13], in which proton (deuteron) pair or cluster wave function becomes near Gaussian type distribution and fusion rate is estimated by the Fermi's first golden rule, while plasma or beam-target type fusion reaction takes place as two-body collision process of plane (free particle) wave functions within an impulse short time interval and its reaction rate is estimated by the Fermi's second golden rule (collision/reaction cross section times free particle flux) [13]. Rate estimation of cold fusion by the collision process drastically underestimates fusion reaction rates, due to the neglect of life-time of trapped particles and very enhanced wave function overlap of multi-body cluster particles that are co-existing in a trapped potential [13].

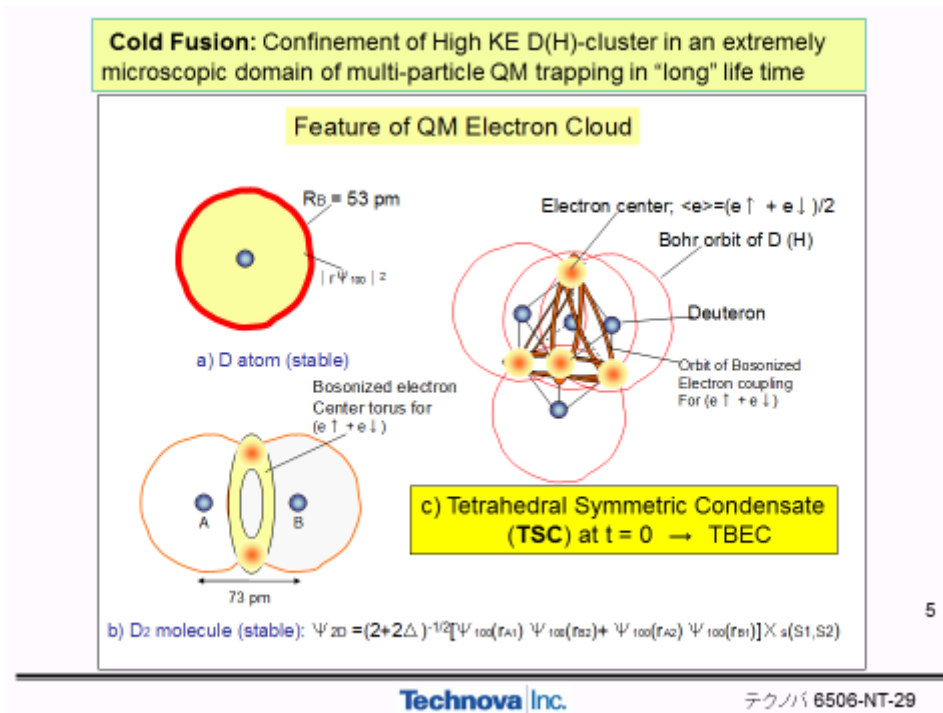


Fig.2: Image of electron cloud for H(D)-atom, H<sub>2</sub>(D<sub>2</sub>) molecule and 4H(D)/TSC

H(D) cluster trapping potential is born by Coulombic interaction between positive charge protons (deuterons) and negative charge electrons. Basic solution for H(D) atom and H<sub>2</sub>(D<sub>2</sub>) molecule are well known, as seen by electron cloud image in Fig.2.

In the QM Langevin calculation, we apply the quantum-mechanical ensemble averaging of physical observables using the weight functions of electron wave-function and particle (p or d) wave function. The case of D<sub>2</sub> (same with H<sub>2</sub>) is shown in Fig.3, adopting Born-Oppenheimer wave-fuction separation between deuteron-pair (or same for proton pair) and electrons.

**Quantum-Mechanical Ensemble-Averaging**

$$\langle G \rangle_{ensemble} = \langle \Psi | G | \Psi \rangle$$

Born-Oppenheimer Approximation for H<sub>2</sub> molecule:

$$\Psi(R_{dd}; r_{A1}, r_{A2}, r_{B1}, r_{B2}) = \Psi_{2D} \cdot X(R_{dd})$$

Electron Wave Function for H<sub>2</sub>:

$$\Psi_{2D} = \frac{1}{\sqrt{(2+2\Delta)}} [\Psi_{100}(r_{A1})\Psi_{100}(r_{B2}) + \Psi_{100}(r_{A2})\Psi_{100}(r_{B1})] X_z(S1, S2)$$

Proton-Pair Wave Function: Gaussian approximation:

$$X^2(R'_{dd}; R_{dd}(t)) = \frac{1}{\sqrt{2\pi\sigma^2}} \exp[-(R'_{dd} - R_{dd}(t))^2 / (2\sigma^2)]$$

6

---

Technova Inc. テクノバ 6506-NT-29

Fig.3: Image of QM ensemble averaging with H<sub>2</sub> (D<sub>2</sub>) wave functions

The p-p pair (or d-d pair) trapping potential (by electron cloud) is Vs2(1,1) function [7, 9, 10, 11]. The Heitler-London type analytical solution of Vs2(1,1) potential contains difficult mathematical function (exponential integral) when we will apply the heavy mass electronic quasi-particle (HMEQP) potentials as pseudo potentials of time-dependent TSC (tetrahedral symmetric condensate) trapping potentials, as described by the HMEQPET method [10, 11, 13]. In this work, we adopt Vs1(1, 1.41) potential as an approximate pseudo-potential for H<sub>2</sub> trapping, as shown in Fig. 4. Later in QM-Langevin code, we extend to use Vs1(m, 1.41) HMEQP potential, with continuously increasing mass m of electron pairs on a face of TSC (having 6 faces) cube and fixed charge of 1.41. Numerical calculation for Vs1(m, 1.41) pseudo-potentials for m = 1 to 1000 has no

difficulty to give regular smooth functions.

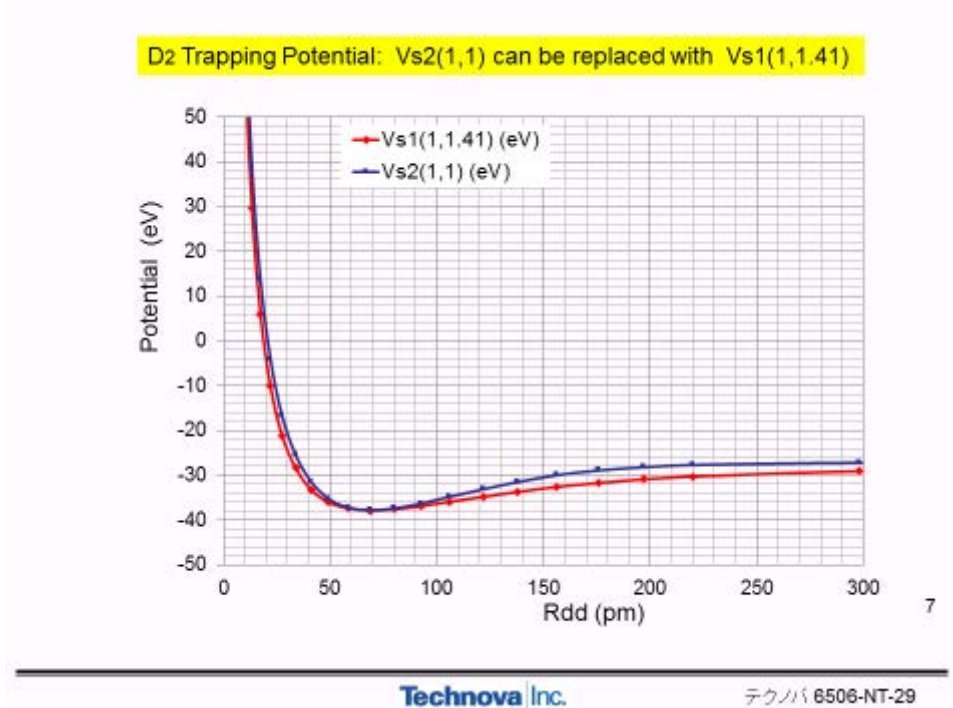


Fig.4 Approximate  $D_2$  ( $H_2$ ) trapping potential  $Vs1(1, 1.41)$  vs.  $Vs2(1,1)$  exact potential

The starting point electron wave function of 4H/TSC ( $t=0$ ) as illustrated in Fig.2 is given by “vector” wave function of Fig.5. On 6 faces of TSC, we have  $H_2$  type electron wave functions. The position vector  $\mathbf{a1}$  through  $\mathbf{a6}$  will make condensation motion for  $t > 0$ . Based on the QM variational principle, we assume that the orthogonally coupled two tetrahedrons of p (d) wave-functions and electron wave functions should form time-dependent energy-minimum state. This state is 4H/TSC ( $t > 0$ ) making condensation/collapse motion, for which we apply the QM Langevin code analysis as shown soon. The condensation motion is calculated for time-dependent variation of p-p (or d-d) distance,  $Rpp$ , assuming the TS (tetrahedral symmetry) configuration as illustrated in c) of Fig.2 or step 1) of Fig.1.

## Wave Function for 4H/TSC (t=0)

$$\begin{aligned} \Psi_{4D} \sim & \mathbf{a1} [\Psi_{100}(r_{A1}) \Psi_{100}(r_{B2}) + \Psi_{100}(r_{A2}) \Psi_{100}(r_{B1})] X_s(S1, S2) \\ & + \mathbf{a2} [\Psi_{100}(r_{A1}) \Psi_{100}(r_{D4}) + \Psi_{100}(r_{A4}) \Psi_{100}(r_{D1})] X_s(S1, S4) \\ & + \mathbf{a3} [\Psi_{100}(r_{A2}) \Psi_{100}(r_{C4}) + \Psi_{100}(r_{A4}) \Psi_{100}(r_{C2})] X_s(S2, S4) \\ & + \mathbf{a4} [\Psi_{100}(r_{B1}) \Psi_{100}(r_{D3}) + \Psi_{100}(r_{B3}) \Psi_{100}(r_{D1})] X_s(S1, S3) \\ & + \mathbf{a5} [\Psi_{100}(r_{B2}) \Psi_{100}(r_{C3}) + \Psi_{100}(r_{B3}) \Psi_{100}(r_{C2})] X_s(S2, S3) \\ & + \mathbf{a6} [\Psi_{100}(r_{C3}) \Psi_{100}(r_{D4}) + \Psi_{100}(r_{C4}) \Psi_{100}(r_{D3})] X_s(S3, S4) \end{aligned}$$

6-Bonds of "Bosonized" electron-pairs ( $e\uparrow + e\downarrow$ ), which forms  
**Regular Tetrahedron (PA)** PA: Platonic Arrangement  
 4-Electron-Centers at Vertexes of **Regular Tetrahedron (PA)**  
**6 faces (Nf=6) and 6 edges (Ne=6)**

$$u_{1s1}(r) = \Psi_{100}(r) = (1/\pi)^{1/2} (1/a_B)^{3/2} \exp(-r/a_B)$$

8

Technova Inc.

テクノバ 6506-NT-29

Fig.5: Image of starting 4H/TSC electron wave-function

The QM Langevin equation [7, 10, 11] is of force balance equation for 6 edges of TSC configuration under the 'friction' (or balance force) of electrons cloud and QM fluctuation of 4H(D) TS configuration [10, 11]. This is a kind of stochastic differential equation. Up to now, we have treated only the motion of expectation value of Rpp (R in Fig.6). The QM Langevin equation for expectation value of p-p pair distance is derived by the ensemble averaging with Gaussian type p-p pair density function as shown in Fig.6. The averaging for electron QM density function results in the friction term as shown in Fig.7. Some more discussions are given for the friction term in Reference [7]. In this paper, we adopt time-dependent friction term of HMEQ p-e\*-p type trapping pseudo potential on

**QM Average of Langevin Equation for D(H) Cluster**

$$N_e m_d \frac{d^2 R}{dt^2} = -\frac{k}{R^2} - N_f \frac{\partial V_s}{\partial R} + f(t)$$

$N_e$ : Number of p-p edges  
 $N_f$ : Number of faces

$$N_e m_d \left\langle \Psi(R, R') \left| \frac{d^2 R}{dt^2} \right| \Psi(R, R') \right\rangle = - \left\langle \Psi(R, R') \left| \frac{k}{R^2} \right| \Psi(R, R') \right\rangle$$

$$- N_f \left\langle \Psi(R, R') \left| \frac{\partial V_s}{\partial R} \right| \Psi(R, R') \right\rangle + \langle \Psi(R, R') | f(t) | \Psi(R, R') \rangle$$

$$\Psi(R, R') = \frac{1}{\sqrt{2\pi\sigma^2}} \exp(-(R'-R)^2 / (2\sigma^2))$$

Gaussian Wave Function

$$N_e m_d \frac{d^2 \langle R \rangle}{dt^2} = -\frac{k}{R^2} - N_f \frac{\partial V_s}{\partial R} + \langle f(t) \rangle$$

Equation for Expectation Value

10

---

Technova Inc.      テクノバ 6506-NT-29

Fig.6: Treatment of QM ensemble averaging of Langevin equation with Gaussian wave-function of p-p pair density

**QM-Average for Complex H-cluster under Platonic Symmetry**

- Average on Electron-wave function is replaced with Friction (Constraint) as

$$\langle Constraint \rangle_{electron-wave} = -N_f \frac{\partial V_{si}(R_{dd}; 1, 1)}{\partial R_{dd}}$$

$N_f$ : Number of faces for Platonic polyhedron  
 $V_{si}$ :  $H_2$  ( $i=2$ ) or  $H_2^+$  ( $i=1$ ) trapping potential  
 **$V_{s1}(m, Z)$  EQPET potential for TSC dynamics**

- Average on p-p wave function: using

$$\Psi(R, R') = \frac{1}{\sqrt{2\pi\sigma^2}} \exp(-(R'-R)^2 / (2\sigma^2))$$

9

---

Technova Inc.      テクノバ 6506-NT-29

Fig.7: Treatment of p-p pair constraint by electron cloud

each face of 6 TSC faces with e-e anti-parallel electron spin pair. The pseudo potential is

approximated by  $Vs1(m, 1.41)$  with quasi fermion  $e^*(m, 1.41)$ . In the calculation  $m$  is related to the time-dependent change of  $R_{pp}$  by the HMEQPET method [11, 10].

The QM Langevin equation is non-linear to  $R_{pp}$  variation, and very difficult to solve analytically. We have introduced a computation program [7] for numerical simulation based on the Verlet's method which solves coupled difference equations for position and velocity as shown in Fig.8.

**Verlet's Method**

$$G(r,t) = \frac{1.975}{m_d [R(0) - r(t)]^2} + \frac{1}{m_d} \frac{\partial V_s(R_{dd}; m, Z)}{\partial R_{dd}}$$

$$R_{dd}(t) = R_0 - r(t)$$

$$\frac{d^2 r(t)}{dt^2} = G(r,t)$$

$$r(t + \Delta t) = r(t) + v(t)\Delta t + \frac{1}{2} G(r,t)(\Delta t)^2$$

$$v(t + \Delta t) = v(t) + \frac{\Delta t}{2} [G(r,t + \Delta t) + G(r,t)]$$

For 4D/TSC with sigma 0.39  
Different value for other cluster

Technova Inc.      テクノバ 6506-NT-29

Fig.8: The non-linear QM Langevin equation is numerically computed by the Verlet method

If  $G(r,t)$  becomes constant, the equation becomes usual Newtonian equation of classical mechanics. For the TSC motion,  $G(r,t)$  is non-linear function containing the effect of QM electron cloud and QM fluctuation of TSC configuration term  $\langle F(t) \rangle$ .

### 3. Simulation of 4H/TSC End State Motion

#### 3.1 HME Langevin DDL Code

We have modified the D(H)-Cluster Langevin Code [7] for taking the following conditions into account.



- 1) Adoption of time dependent pseudo-potentials for TSC trapping
- 2) Fix-up of repulsive p-p state at the collapse end state:  $R_{pp} \geq 2.4$  fm
- 3) Taking relativistic effect for electron state (imitating so called DDL component [8])

The flow chart of HME Langevin DDL Code is given in Fig.9.

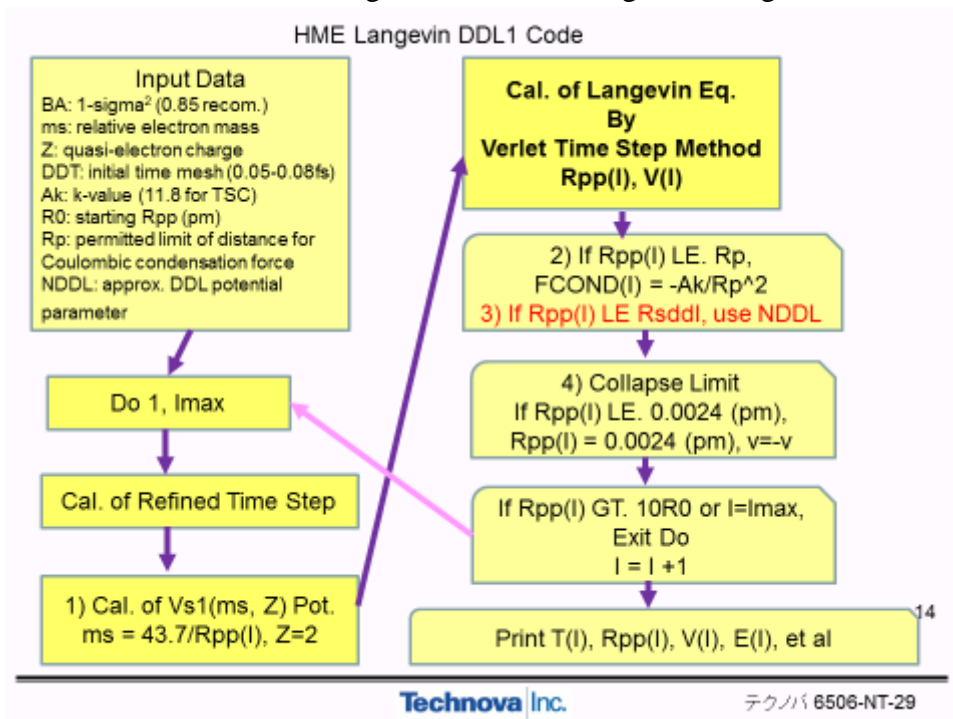


Fig.9: Flow chart of HME Langevin DDL code

Many input parameters should be chosen first:

BA:  $1-\sigma^2$  (0.85 recommended); the sigma parameter defines dispersion of Gaussian type p-p pair wave function. By the variation principle analysis using Schrodinger equation,  $\sigma = 0.49$  is recommended to realize the system energy minimum state in condensing TSC configuration.

ms: relative electron mass; initial value of  $e^*$  mass, 1.0 is used.

Z: quasi-electron charge; relative ratio of  $e^*$  charge and electron charge

DDT: initial time mesh (0.05-0.08fs is recommended)

Ak: k-value (11.8 for TSC); centripetal condensation force term of cluster

R0: starting  $R_{pp}$  (pm); usually 74 pm for TSC and  $H_2$ , and 138 pm for p-e-p system

Rp: permitted limit of distance for Coulombic condensation force;  $R_p = 5.8$  fm is used by considering the limit of e-e QM center distance due to the classical electron radius 2.8 fm.

NDDL: approximated treatment for DDL (deep Dirac level of electron) potential parameter for DDL1 simulation. Potential dip by Gaussian function is used for DDL2

simulation

Time mesh of starting calculation is chosen roughly around 0.05 fs. Calculation of 4H/TSC condensation motion starts with  $R_{pp}(t=0) = 74$  pm, and gets to the collapsed state of  $R_{pp}$ -minimum = 2.4-3 fm in about 1.2 fs (see examples in the following sections). The very drastic decrement of  $R_{pp}$  with ca. 4 orders of magnitude requires the adjustment of time mesh to be much smaller according to the smaller  $R_{pp}$  value, for keeping the accuracy of numerical calculation by the Verlet double difference equation scheme. In the code, time mesh is chosen automatically as the  $R_{pp}$  value of former time step changes. The smallest time mesh at around  $R_{pp} = 3$  fm was on the order of  $1.0E-22$  s.

According the change of  $R_{pp}$  value, pseudo potential of TSC trapping is calculated with  $Vs1(m, Z)$  function [10, 11, 13]. Some examples of  $Vs1(m, Z)$  curves are shown in Fig.10.

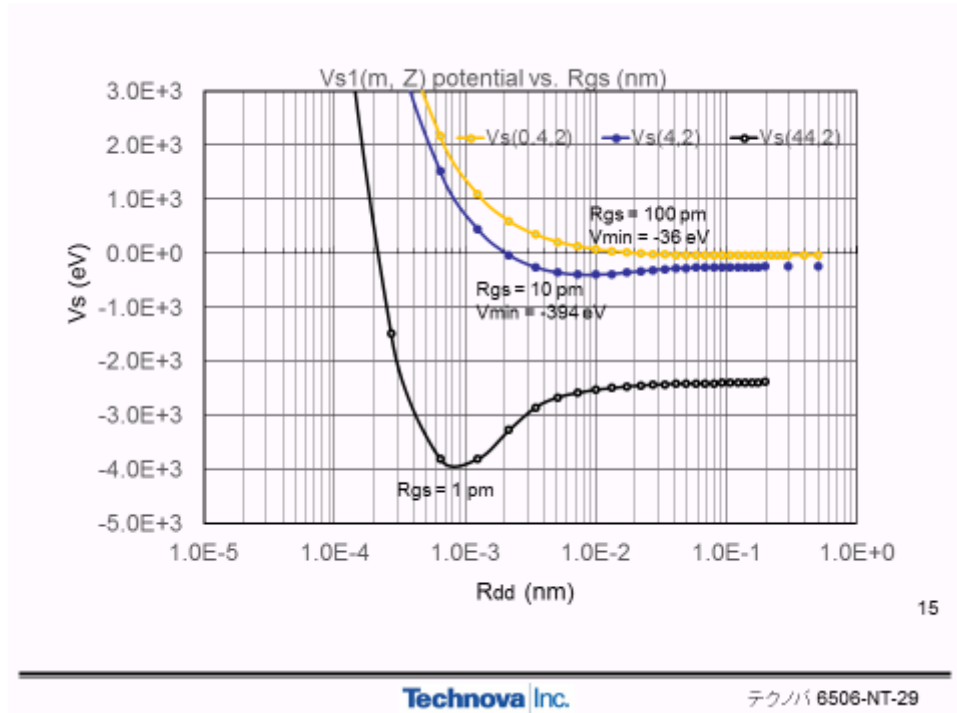


Fig.10: Example of pseudo potentials for TSC trapping [13]

Ground state eigenvalues as energy level and p-p distance are calculated by the variational principle code with Gaussian type wave function [10, 11, 13]. We can make various trial calculations for wide variety of pseudo potentials, by choosing  $(m, Z)$  combination for the quasi-particle  $e^*(m, Z)$ . However, the HMEQPET method is a pure mathematical tool to carry out difficult numerical computation for the very fast condensation/collapse motion of H(D)-cluster which has no ground state than pure time-dependent dynamic motion. Of course, when we apply the MHE Langevin code to steady systems as  $H_2$

molecule,  $H_2^+$  ion, d-muon-d molecule, etc. , we use fixed potential as  $Vs2(1,1)$  or  $Vs1(1, 1.41)$ ,  $Vs1(1,1)$ ,  $Vs1(207,1)$  or  $Vs1(50,2)$ , etc. to meet the periodic ground state oscillations (see some examples in the following sections and Appendix).

Calculated results with the Verlet time step method with various input conditions are shown in the following sections. First, we will check features of 4H/TSC motion with MHEQ pseudo potentials. Next we try very rough treatment of DDL (deep Dirac level) effect in trapping potentials. Lastly, we apply MHEQ pseudo potentials and Gaussian type trapping dip component by DDL effect, for simulation of 4H/TSC end state oscillation.

### 3.2 Examples with $Vs1(m,1)$ pseudo potentials without DDL effect

In Fig.11-1 and Fig.11-2, calculated results of  $Rpp(t)$  and  $Epp(t)$  curves are shown. We see ‘strange band structure’ at around 1.5 fs of Fig.11-1. Fig.11-2 shows expanded view of the ‘strange band structure’, where we find 6 chaotic oscillations. Minimum  $Rpp$  values are all 2.4 fm that is the value of hard core limit of p-p distance. Due to the adoption of  $v = -v$  (velocity inversion) fix up condition at  $Rpp = 2.4$  fm, motion bounces there and oscillates chaotically. Maximum relative kinetic energy of p-p pair is ca. 200 keV.

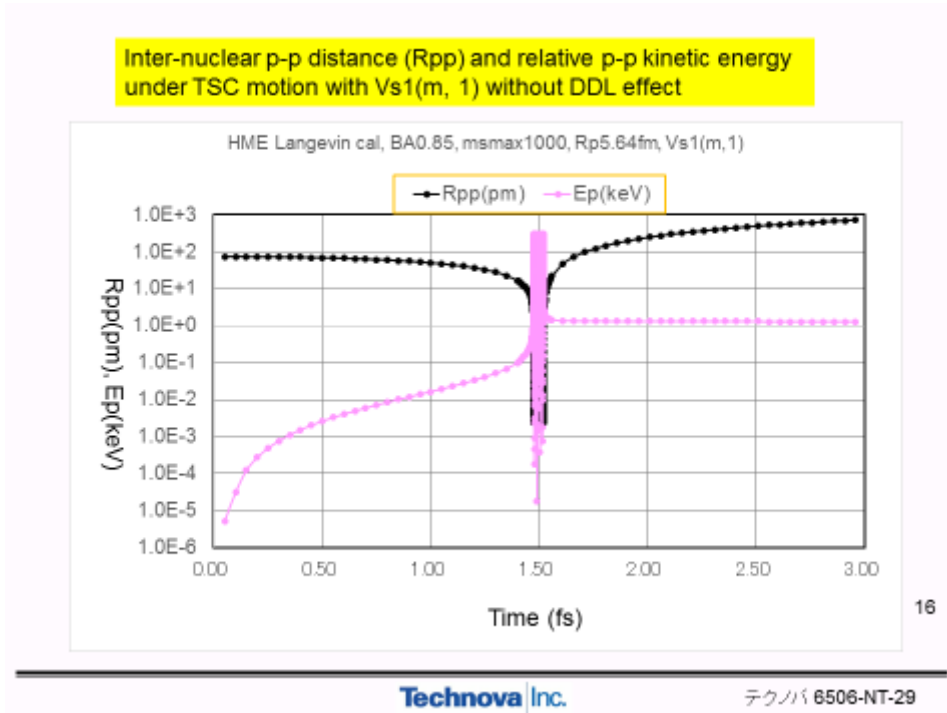


Fig.11-1: Inter-nuclear p-p distance ( $Rpp$ ) and relative p-p kinetic energy draw strange view of band structure-like graphs, for 4H/TSC condensation/collapse motion simulation with  $Vs1(m,1)$  time-dependent TSC trapping pseudo potentials

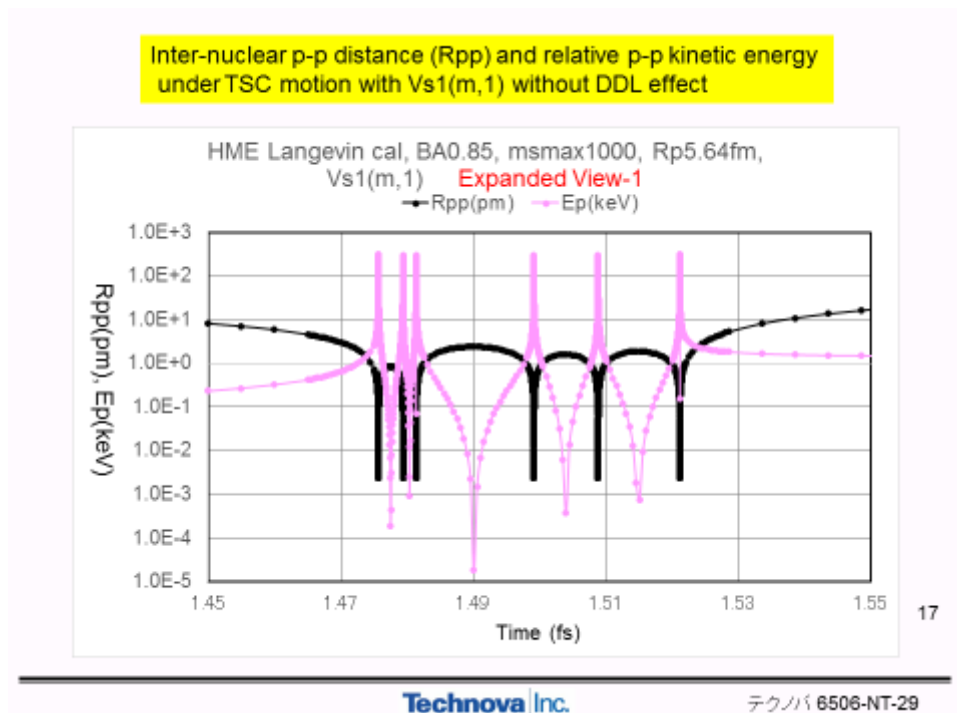


Fig.11-2: Expanded view of the ‘band-like structure’ at around 1.5 fs of Fig.11-1

### 3.3 Simulation Results with Approximate Treatment of DDL Effect

Muelenberg-Paillet’s, M-P (at the ICCF19 meeting [8], and private communication), DDL-combined potential has a p-p trapping dip ( $\sim 100\text{keV}$  depth?) at around 2-5fm of  $R_{pp}$ , where total p-p repulsive energy is around 200 keV. This means that a p-p with relative kinetic energy larger than 200 keV will be trapped there, at least for a while.

Here DDL is acronym of Deep Dirac Level for electron orbit as given as the Dirac equation solution first reported by J. A. Maley and J. Va’vra (submitted to Fusion Technology, 24, 1993).

For usual non-relativistic QM solution ( $E_0$  term by M-P: see Fig.12),  $R_{pp}(gs) = 138$  pm with negative potential well of  $E_0$  term or  $Vs1(1,1)$  potential, with relative p-p kinetic energy ca. 1 eV. So that, usually known  $H_2^+$  ion wave function may have negligibly small component at the A term dip (DDL-related femto-molecular state).

However, when relative p-p kinetic energy exceeds ca. 100 keV, in some dynamic p-p transient motion like 4H/TSC, a p-p pair will be trapped in the dip, for some definite time interval with enhanced transition via QM tunneling effect from the 138 pm p-e-p system ground state. Above slides in Section 2.2 show time-dependent behavior of 4H/TSC motion, making condensation/collapse/disruption (scattering), calculated by the HME Langevin code without the DDL term. The HME Langevin code utilizes  $Vs1(m, Z)$

pseudo-potential, in time (or  $R_{pp}$ )-dependent way. It has a fix-up of contraction limit at  $R_{pp} = 2.4$  fm (twice of proton radius): this makes a primitive way of particle scattering at  $R_{pp} = 2.4$  fm. And twice the electron classical radius  $2.82$  fm was used for the limitation ( $R_p/2$ ) of condensation force. Calculated relative p-p kinetic energy at around  $R_{pp} = 2.4$  fm is ca. 200 keV, where we see interesting several oscillations of p-p distance and electron p-p kinetic energy.

The author understands the M-P work looks reasonable and is important for CMNS solvers. The work should be encouraged. In the following, some trial calculations by the HME Langevin DDL1 code (modified version of the D(H) Cluster Langevin code) are shown with simplified approximate potential change for the DDL effect, using parameter NDDL. With NDDL=2, we set it for the case without the DDL effect. With NDDL = 1.5-1.7, we make simplified corrections for DDL effect. See Fig.12 for getting idea of this rough treatment for the P-M type DDL effect in trapping potentials.

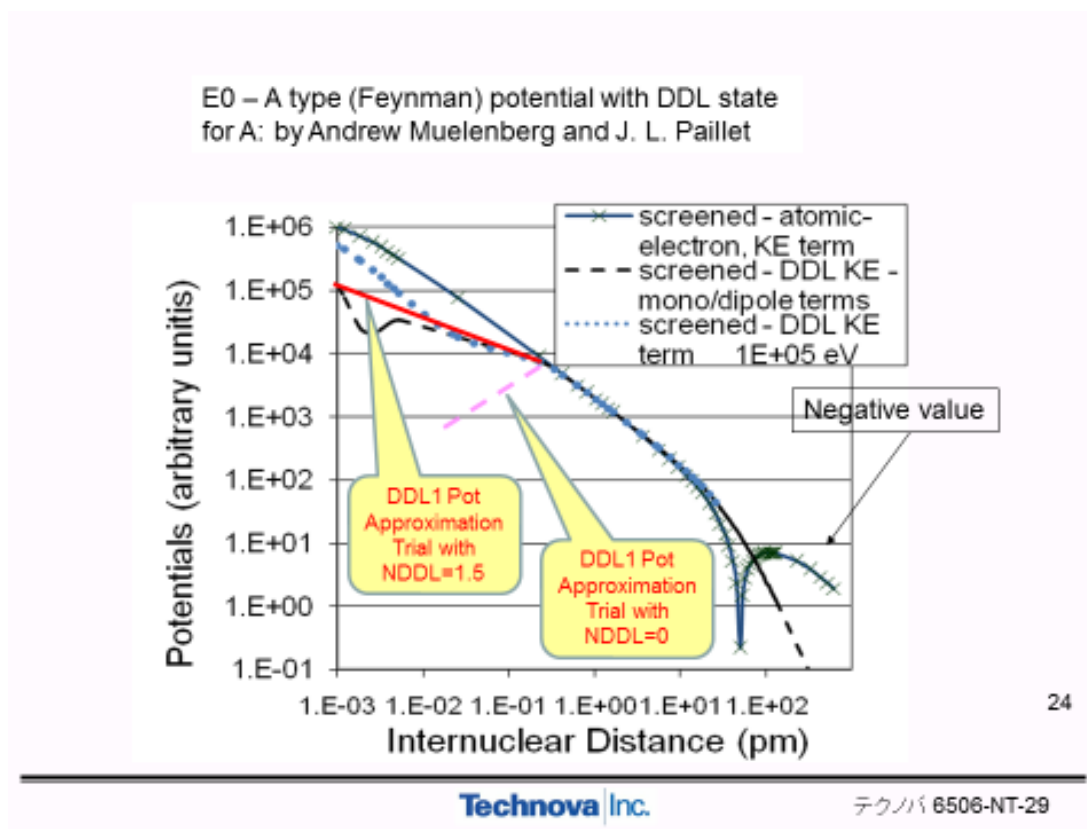


Fig.12: Deep Dirac level (DDL) components estimated by Muelenberg-Paillet [8] and rough parameter NDDL to fit the modification of  $V_{s1(1,1)}$  type p-e-p system potential

The  $V_{s1(1,1)}$  type p-p trapping potential has negative valley (bottom at around 130 pm),

which is drawn here with positive hump, because of logarithmic vertical scale of figure. M-P have modified original non-relativistic  $Vs1(1,1)$  type potential with non- $1/R$  function component in Fig.12.

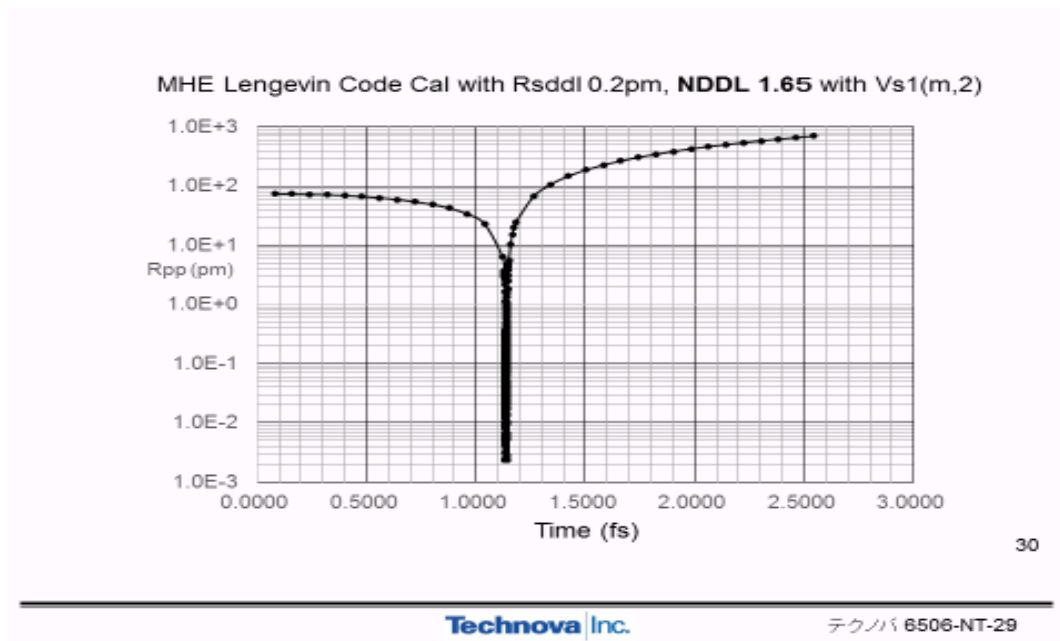


Fig.13-1: Simulation of 4H/TSC condensation collapse motion with DDL1 effect and  $Vs1(m,2)$  time-dependent pseudo potentials;  $Rsddl = 0.2$  pm,  $NDDL = 1.66$

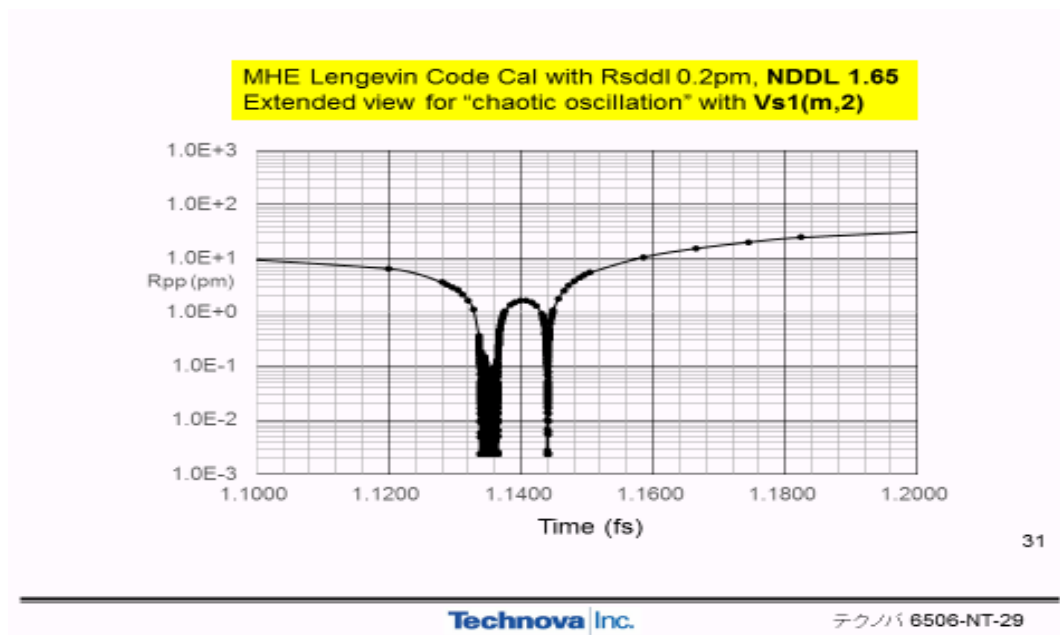


Fig.13-2: Extended view of Fig.13-1 at around time region of 1.14 fs

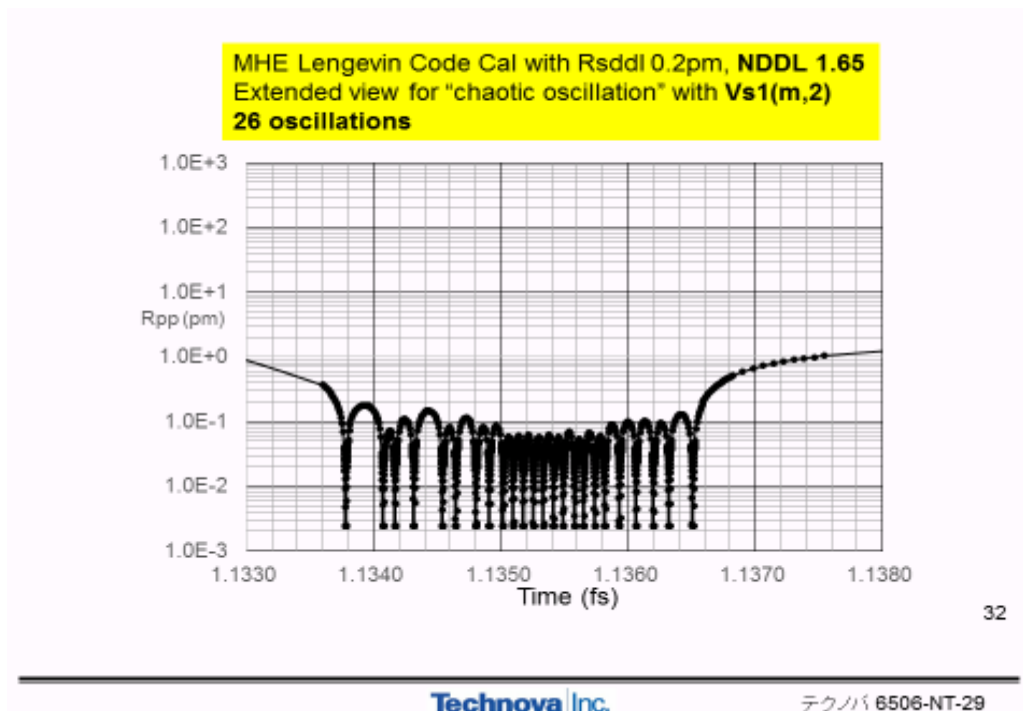


Fig.13-3: Extended view of Fig.13-2 in the time region near 1.135 fs

By adopting  $NDDL = 0$ , we have surely get the end state eternal trapping of 4H/TSC at  $Rpp = 2.4$  fm. It is confirmed by our real simulation by the MHE Langevin DDL code, but the graph is too trivial to show here.

Typical example of chaotic end state oscillation appeared by the simulation is shown in [Fig.13-1](#), [Fig.13-2](#) and [Fig.13-3](#), by using DDL effect parameters of  $Rsddl = 0.2$  pm (starting distance of DDL effect correction),  $NDDL = 1.66$  with main trapping potential of  $Vs1(m, 2)$ . Chaotic end state oscillation appeared with  $Rpp$  max of around 100 fm and  $Rpp$  min of 2.4 fm for 30 cycles (See Fig. 13-3), and got out to the second group oscillation at around 1.144 fs from which TSC cluster was kicked out to disruption.

Another typical chaotic oscillations are shown in [Fig.14-1](#), [Fig.14-2](#) and [Fig.14-3](#), by using DDL parameters of  $Rsddl = 0.2$  pm and  $NDDL = 1.666$  with  $Vs1(m, 2)$  potentials. In this case strange band structure appeared at around 1.135 fs. Variation of amplitudes and intervals (frequency) of oscillation showed chaotic change. The end state chaotic oscillation continued for about 0.008 fs with 32 oscillations with amplitude change between 2.4 fm to ca. 100 fm.

By changing DDL parameters, many calculations were tried. For many cases, we observed single collapse-and-bouncing-out events, as summarized in [Fig.15](#) for the change of  $NDDL$  parameter, and in [Fig.16](#) for the change of BA (Gaussian width

dependence of p-p wave function) parameter.

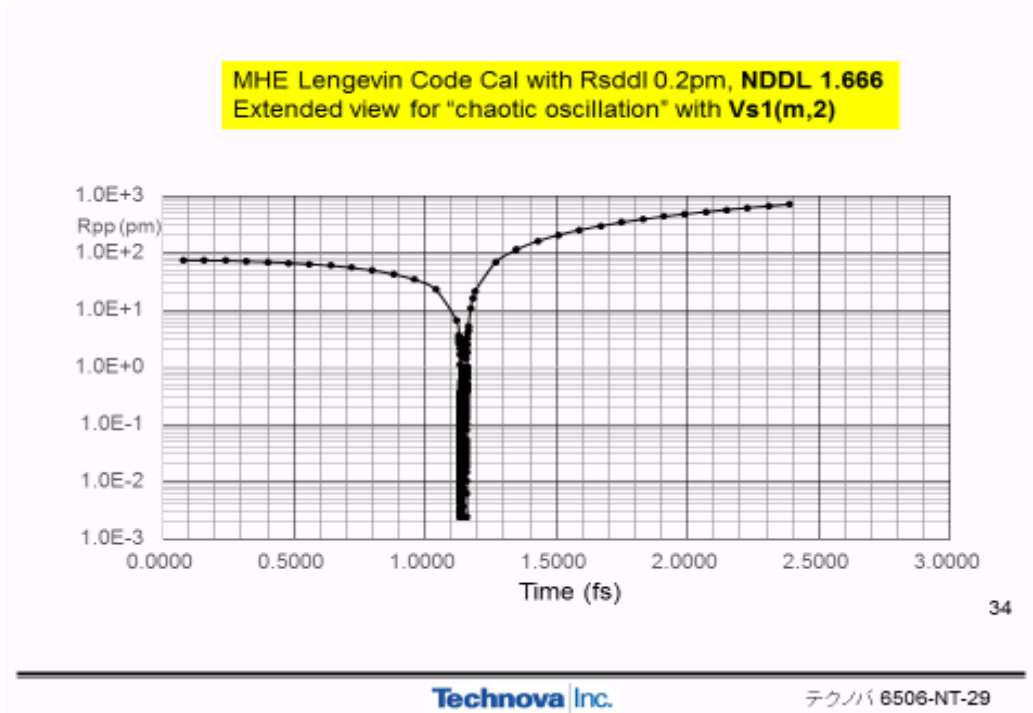


Fig.14-1: Simulation of 4H/TSC condensation collapse motion with DDL1 effect and Vs1(m,2) time-dependent pseudo potentials; Rsddl = 0.2 pm, NDDL = 1.666

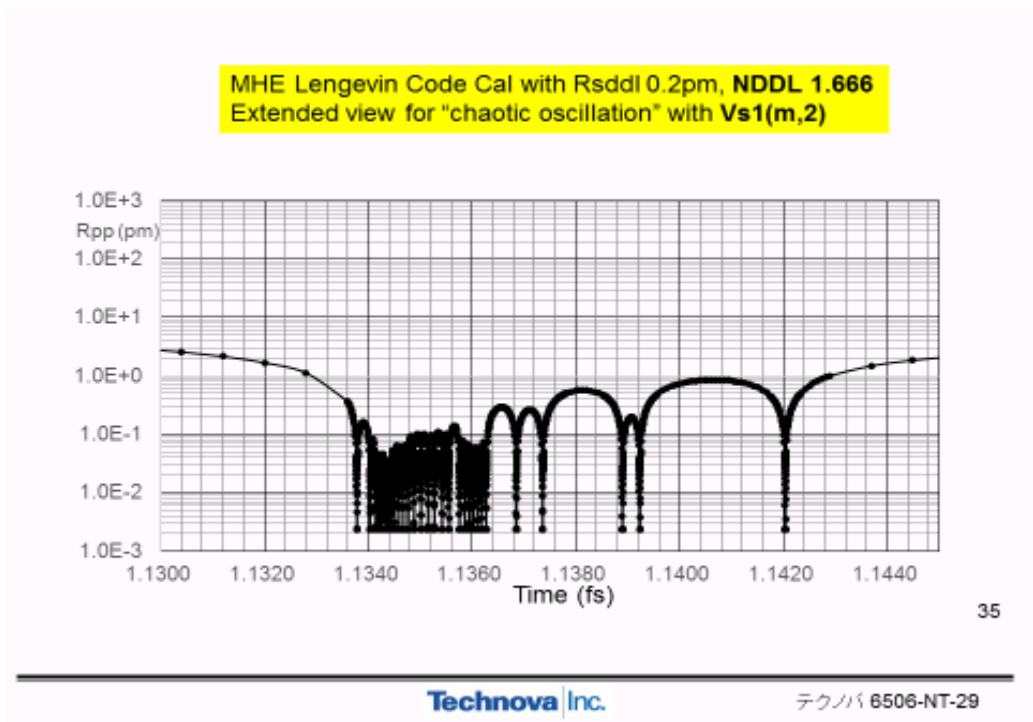


Fig.14-2: Extended view of Fig.14-1 near around 1.135 fs



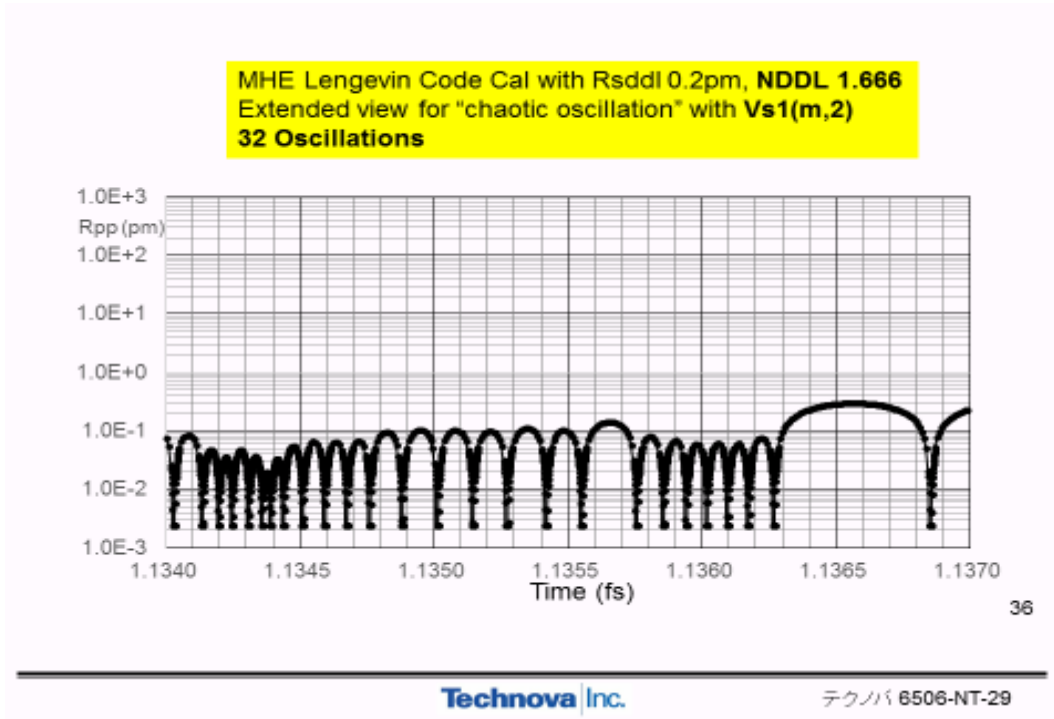


Fig.14-3: Extended view of Fig.14-2 near around 1.1355 fs

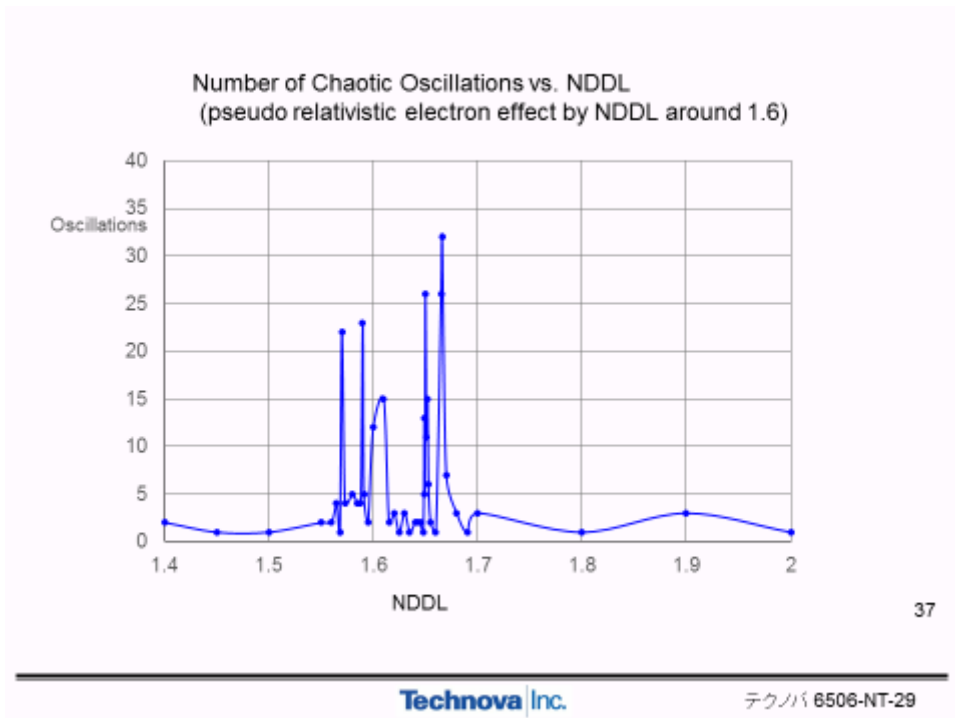


Fig.15: Occurrence of chaotic end state oscillation as the change of NDDL parameter

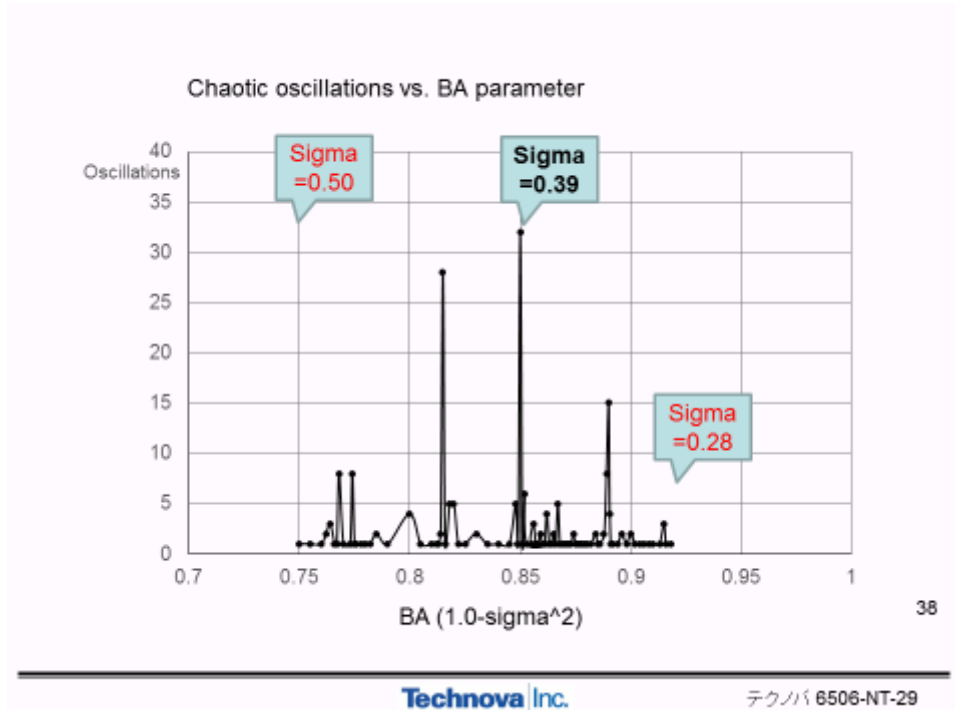


Fig.16: Change of chaotic end state oscillation as the change of p-p wave function dispersion

### 3.4 Simulation with Gaussian type DDL Dips

Fig.17 is copied after the Muelenberg-Paillet presentation/paper to ICCF19 [8]. They considered the DDL level appears at  $R_{pp} = \text{ca.}1.2$  fm, namely inside the proton three quark core. This is too extreme in the view of nucleon structure and strong interaction. The author made modification with milder electron relativistic level dip on the main  $V_{s1}$  type trapping potential. Modification of potential was done with Gaussian type dip function by the DDL effect (DDL2 calculation):

- $V_s(r) \rightarrow V_s(r)(1-f(r))$  ; modified p-p trapping potential with DDL level
- $f(r) = A \exp(-(r-R_{ddl})^2/(\sigma R_{ddl}^2))$ ; Gaussian type dip function
- $R_{ddl} = 5$  to  $20$  fm ;local pot minimum point
- $\sigma = 0.3$  to  $0.6$ ; dispersion of Gaussian dip
- $R_{sddl} = 200$  fm ;starting p-p distance for DDL correction
- $A = 130/144$  ;weight of Gaussian type DDL dip correction

An example of modified potential curve with the DDL level correction is shown in Fig.18.

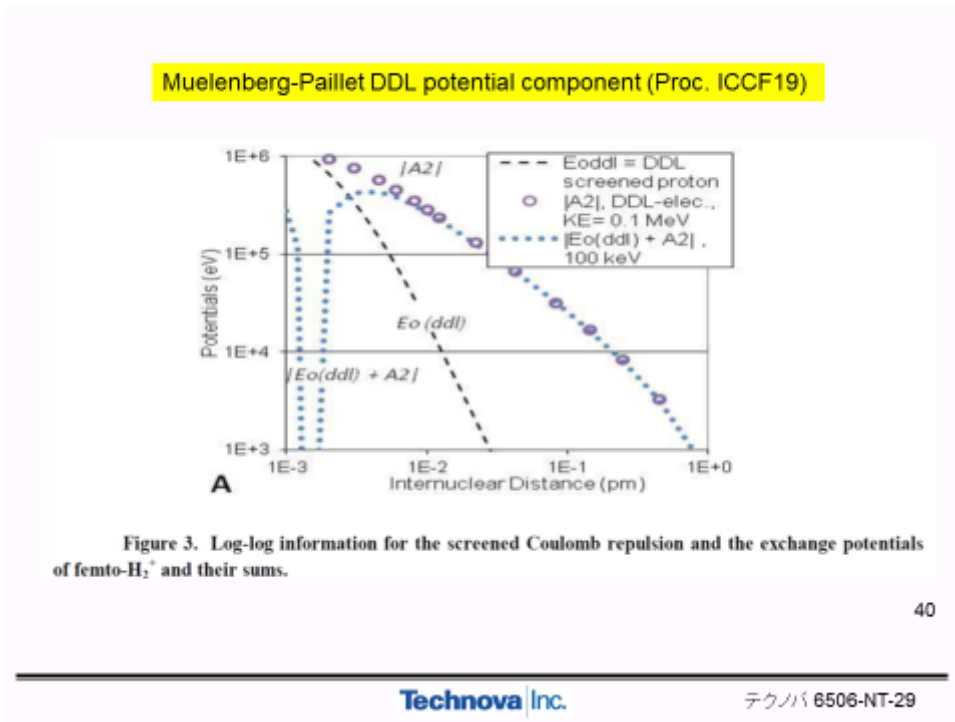


Fig.17: Potential dip by DDL level for main p-e-p trapping potential, by Muelenberg-Vaillet [8]

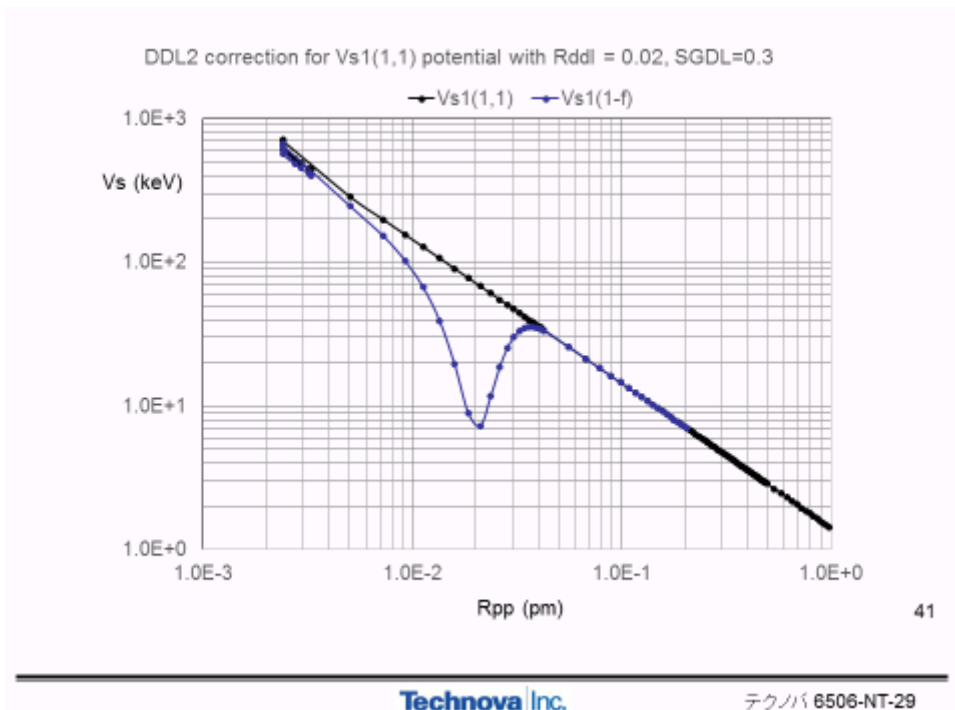


Fig.18: Example of DDL level correction (modification) for  $V_{s1}(1,1)$  potential

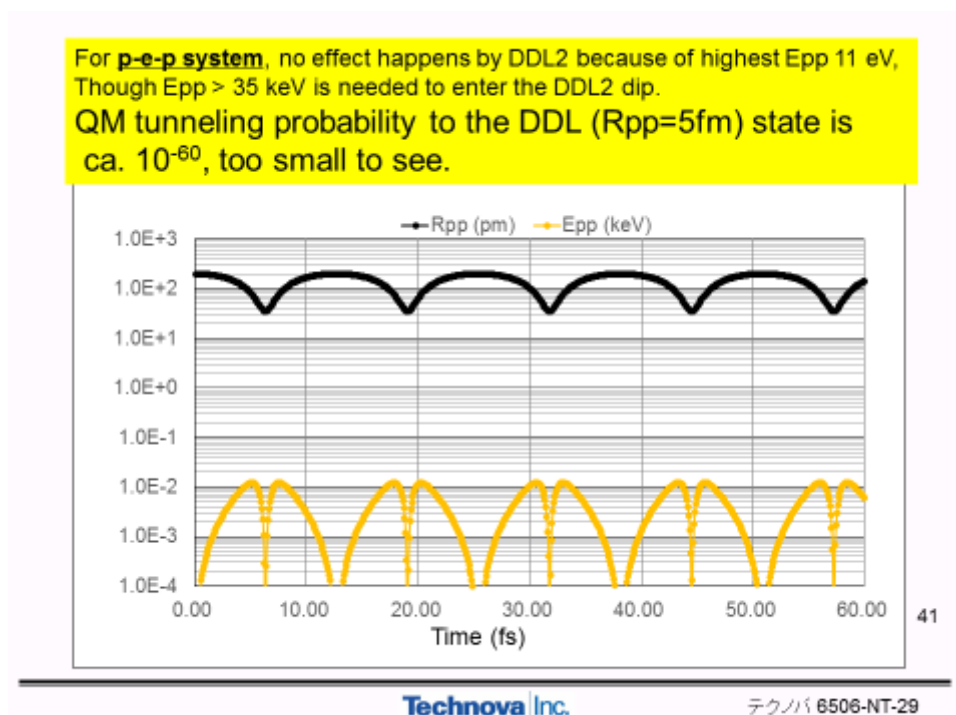


Fig.19: Simulation of dynamic motion of p-e-p system with DDL2 component

For a trial check calculation, simulation of dynamic motion for a p-e-p ( $H_2^+$  ion molecule) three body system was done with the DDL contained potential of Fig.18. Results are plotted in Fig.19. Periodic ground state oscillation of p-e-p system is calculated, and we do not see any effect of DDL level dip of trapping potential. Since the maximum p-p kinetic energy is calculated as 11 eV, classical mechanics prevents p-p pair to get in the DDL level after trapping potential height (barrier) of 35 keV (see Fig.18). Quantum mechanically, there exists tunneling transition probability from the minimum p-p distance to the DDL level ( $R_{ddl} = 20$  fm in this case). However the tunneling probability is calculated (see method in [13]) to be ca.  $1.0E-60$ , namely negligibly small.

We can conclude the assumed DDL level do not make diminished size p-e-p molecule and the ground state of p-e-p system with  $R_{pp}(\text{gs}) = 138$  pm does not have visible change from the usual  $V_{s1}(1,1)$  potential QM state. Hydrogen exists as molecule ( $H_2$ ) in nature, so that the DDL level obtained from the Dirac equation solution has no real effect on binding energy and inter-nuclear p-p distance. However, when atomic  $H^+$  ion makes recombination with electron, X-ray emission by DDL level transition should happen in nature. Such X-rays (ca. 500 keV?) has never been observed. This means that the assumed DDL state at H-atom must be a tiny QM component that is difficult to observe, even if DDL exists at all in QM relativistic equation solutions.

In Fig.20, we show a typical case of rather stable end state oscillation which was

obtained by simulation with  $R_{ddl} = 20$  fm and  $V_{s1}(m, 1.41)$  potential for a face of 4H/TSC under time dependent motion. After 1.185 fs, rather stable oscillation with amplitude change from 3 fm to ca. 100 fm seems to continue. Due to the limitation of PC memory size, calculation stopped at ca. 1.1855 fs. However, the near stable trend of oscillation suggests further continuation of slowly changing oscillation amplitude and span. The near stable oscillation may continue for more than 1 fs. 320 oscillations were seen in a time interval of 0.04 fs with amplitude (p-p distance) change from 3 fm to ca. 100 fm, and far more oscillations are foreseen to continue due to the rather stable continuation of chaotic oscillation. The state may be classified as a strange attractor of chaos science.

Similar near steady chaotic oscillations are calculated for so many cases of trials with the following band of parameters (graphs were given in the JCF16 presentation):

- HME Langevin DDL2 code with  $N_e=N_f=6$   
 $R_{ddl}$ : 5 to 20 fm  
 Sigma of p-p wave-function: 0.36 to 0.95  
 BA: 0.87 to 0.10  
 Sigma of DDL2 potential: 0.32 to 0.58  
 AW (weight of DDL2 component): (120 to 144)/144 (= 0.83 to 1.0)  
 Minimum Rpp varied from 3.0 fm to 16 fm.

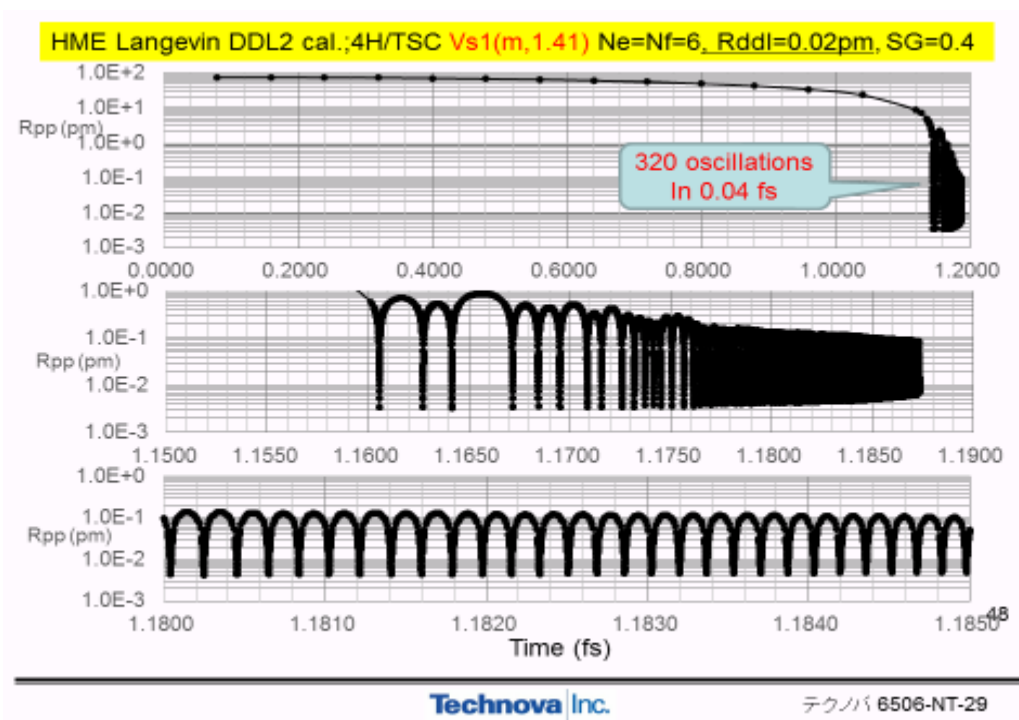


Fig.20: Near steady oscillation (strange attractor of chaos) of end state motion of 4H/TSC, by MHE Langevin DDL calculation with  $V_{s1}(m, 1.41)$  pseudo potential and Gaussian dip

of DDL level

To compare with these near steady but chaotic oscillation, condensation motion of muon stuck d-d-muon molecule behaves smooth decrement of d-d distance and goes to ground state periodic oscillation in 8.3 fs [7], as given some graphs in Appendix.

As discussed in the past papers on WS fusion of 4H/TSC [4-6], possible life time more than 1 fs for the end collapse state of 4H/TSC-minimum may induce ca. 200 W/mol-Ni level WS fusion rate ( $^3\text{He}$ , d, p are products) and significant amount of 4H + Ni process fission products as mostly stable isotopes [4]. To this respect, what the present simulation calculation shows, namely the near steady chaotic end state oscillation, is encouraging consequence of the TSC theory on the Ni-H type CMNR experiments claiming anomalous excess heat generation [1-3].

#### 4. Conclusion

Simulation of end state 4H/TSC oscillation was tried by using several conditions for kick-back at  $R_{pp}=2.4\text{fm}$ , electron condensation limit of classical radius,  $V_{s1}(m,Z)$  pseudo potential for TSC trapping potential ( $V_{tsc}$ ), and relativistic electron potential (DDL) component. Major results are:

- Generation of chaotic oscillation as strange attractor was observed.
- Near Stable Oscillations (may last  $> 1\text{fs}$ ) were found for 4H/TSC with  $V_{s1}(m, 1.41)$  potentials for a wide band of parameters (BA, SGDL, AW).
- Heat power level of more than 200 W/mol-Ni for Ni-H type CMNR experiments can be explained by the enhanced WS fusion by the 4H/TSC end-state oscillation

#### Acknowledgment

The author acknowledges his Technova colleagues, especially Dr. Akira Kitamura and Ms. Reiko Seto for their kind support.

## References:

- [1] A. Kitamura, A. Takahashi, R. Seto, Y. Fujita, A. Taniike, Y. Furuyama; Proc. JCF14 (2014) 1-13.
- [2] A. Kitamura, A. Takahashi, R. Seto, Y. Fujita, A. Taniike, Y. Furuyama; J. Cond. Matt. Nucl. Sci. 15 (2015) 231-239.
- [3] A. Kitamura, A. Takahashi, R. Seto, Y. Fujita, A. Taniike, Y. Furuyama; Proc. JCF15 (2015) 1-19.
- [4] Akito Takahashi: Physics of Cold Fusion by TSC Theory, J. Phys. Sci. Application, 3(3) (2013) 191-198
- [5] Akito Takahashi: Nuclear Products of Cold Fusion by TSC Theory, J. Cond. Matt. Nucl. Sci., 15 (2015) 11-22
- [6] Akito Takahashi: 4H/TSC Fusion Simultaneous Weak and Strong Interactions, Proc. JCF-12, pp.115-127 (2012)
- [7] A. Takahashi, D. Rocha: D(H)-Cluster Langevin Code and Some Calculated Results, Proc. JCF-14, pp.113-140 (2014)
- [8] A. Meulenberg, J. L. Paillet: Basis for Femto-Molecules and Ions Created from Femto-Atoms, Proc. ICCF19, to be published in J. Cond. Matt. Nucl. Sci., in 2016
- [9] Akito Takahashi: Background for Condensed Cluster Fusion, Proceedings of JCF15, JCFRS, pp.63-90 (2015) [http://jcf.rs.org/proc\\_jcf.html](http://jcf.rs.org/proc_jcf.html)
- [10] Akito Takahashi: The basics of deuteron cluster dynamics as shown by Langevin equation, American Chemical Society *LENRSB (Low Energy Nuclear Reaction Source Book)* 2 (2009) 193-217
- [11] Akito Takahashi and Norio Yabuuchi: Study on 4D/TSC condensation motion by non-linear Langevin equation, American Chemical Society *LENRSB* 1 (2008) 57-83
- [12] Akito Takahashi: Kinetic Reaction Energy of Cold Fusion, Proc. JCF-12, pp.67-76 (2012)
- [13] Akito Takahashi: Fundamental of Rate Theory for CMNS, Proc. ICCF19, to be published in J. Cond. Matt. Nucl. Sci. (see [http://vixra.org/author/akito\\_takahashi](http://vixra.org/author/akito_takahashi) [13])

### Appendix: Condensation Motion of dd-muon after muon sticking

Using the same MHE Langevin code, we have done a trial simulation for condensation motion of d-e-d molecule after a muon is stuck. Results are shown in Fig.A1 through Fig.A3.

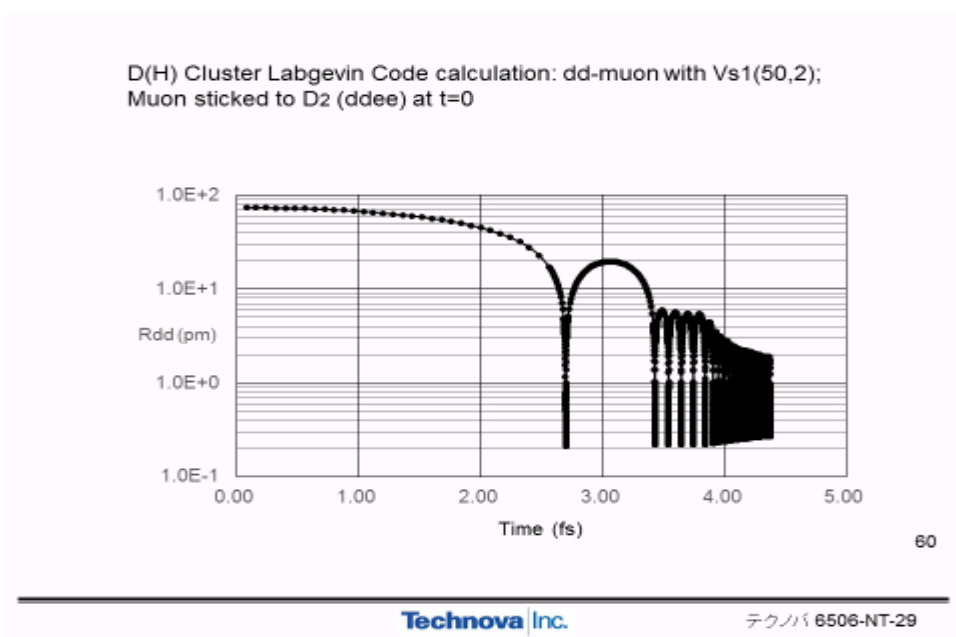


Fig.A1: Simulation of muonic d-d molecule motion after muon sticking at time zero to d-e-d system.

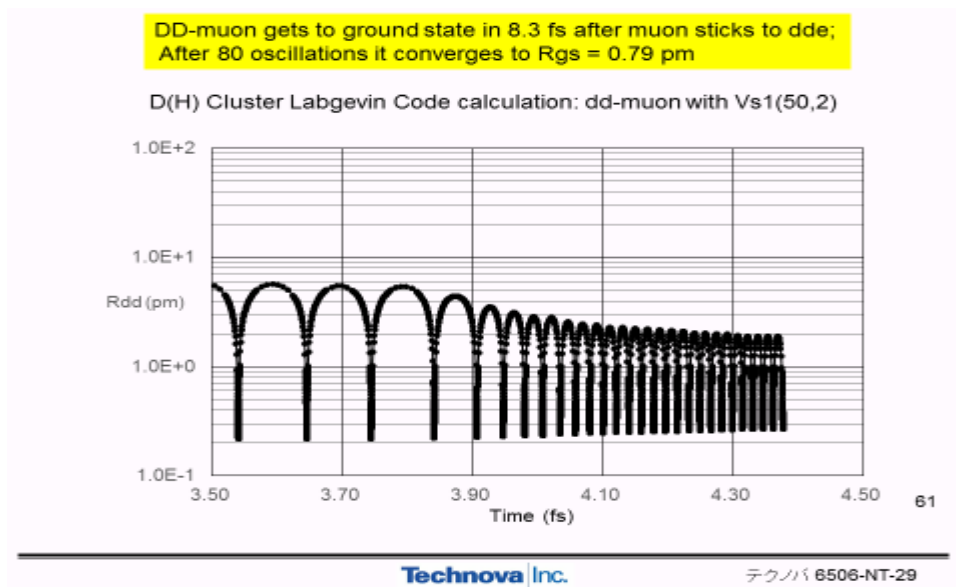


Fig.A2: Expansion of Fig.A1 after 3.5 fs



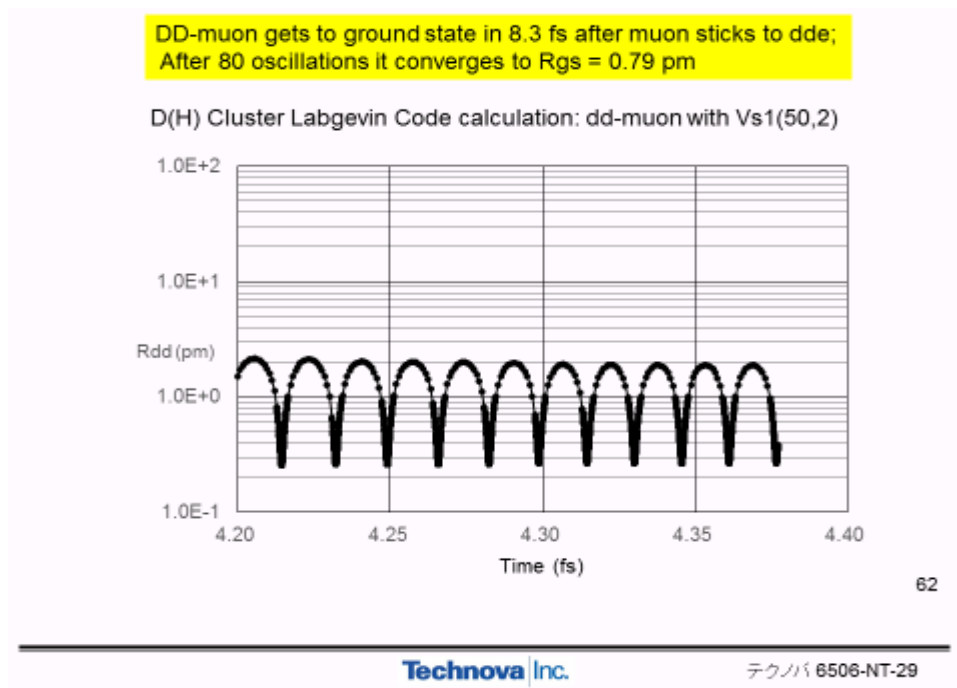


Fig.A3: Expansion of Fig.A2 after 4.2 fs, showing that oscillation is converging to the ground state oscillation smoothly